

COOLER TARGET DEVELOPMENT

1. Overview

F. Sperisen and J. Doskow

The most heavily used target in the Cooler has been the H₂ gas jet. Three experiments (CE-01,¹ CE-08² and CE-23³) have been completed during the past year, and a fourth (CE-03⁴) is currently in production running. For the latter, the jet target had to be moved last December from the G to the T straight section where it was installed just upstream of the 60 spectrometer magnet. The large fringe field of this magnet made it necessary to shield some of the turbomolecular pumps. Other pumps had to be moved out of the high field by connecting them with long tubes to the vacuum chamber. Aside from some other minor modifications, the jet target setup in the T section is quite similar to the one in the G section. For a detailed description see previous reports.^{5,6}

The differential pumping system of the jet target setup has also been used frequently to provide *diffuse* gas targets. This is done by running the gas flow through a needle valve into the 15 cm long central pumping stage. There, the pressure is measured with a capacitance sensor to within about 4 μ Torr (corresponding to 2×10^{12} molecules/cm²). As is the case for the jet, the diffuse target can be switched on/off quickly (and thus synchronized with the Cooler cycle), and its thickness can be controlled remotely. Diffuse targets of various kinds of gases have been used for tests in the experiments mentioned above as well as for luminosity studies⁷ (CE-17) and comparisons with microribbon targets⁸ (CE-18).

Work with microribbon targets has continued over the past year as two experiments (CE-02 and CE-06) require thin, localized carbon targets. To achieve small enough average target thicknesses, the fibers oscillate across the Cooler beam. A year ago we reported on two different methods of fiber oscillation; one by alternating electrical fields,⁹ the other by attaching the ribbons on a spinning disk.¹⁰ Both schemes have since been abandoned in favor of yet another method: The fiber or microribbon is attached to a vibrating frame, suspended by four springs connected to a target holder which in turn can be moved in and out of the beam with a linear motion vacuum feedthrough.¹¹ The frame vibrations are induced by two electromagnets. This oscillating motion proved more stable than the one driven by electric fields, and has the additional important advantage that the average target thickness can be varied easily by changing the amplitude of the oscillation via the amplitude of the driving force. The main problem with fiber targets is not, however, with the method of exposing them to the accelerator beam. Rather, the focus is now on the effect such targets have on the beam lifetime (and thus achievable luminosity) and momentum distribution. Both of these properties seem to be significantly more adversely affected than in the case of (homogeneous) gas targets. The systematic study of these problems is the subject of CE-18, described elsewhere in this report.⁸

In preparation for experiments with polarized Cooler targets (both ³He and polarized hydrogen) we have installed and run two different storage cell targets in the Cooler. The first storage cell, described in last year's report,¹² was installed in August 1990 in the T section for CE-14. It consisted of a copper tube, 28 mm ID, 73 cm long, and cooled to 150 °K. The presence of this cell did not restrict the ring acceptance and posed no problems

for Cooler operation. Lifetimes of 45 MeV proton beams were measured with deuterium and helium targets and incorporated into the CE-17⁷ data base.

More recently, as part of CE-26, another storage cell target has been installed in the A section, downstream of the RF cavity. This cell tube, uncooled, was much narrower (only 8 mm ID) and shorter (24 cm long). A 1.5 μm mylar window made it possible to detect low-energy protons from small-angle pp elastic scattering. Section 2 below describes this setup in some detail. Measurements done with a 185 MeV proton beam and hydrogen and helium targets demonstrated that experiments with storage cells in the Cooler are feasible both in terms of luminosity and clean detection of reaction products. An account of this test is given in a separate contribution¹³ to this report. After another run with a cell of different geometry this summer, we are planning to install the MIT polarized ^3He target for CE-25 in the A section.¹⁴

A recently approved Cooler experiment, CE-19, requires an oxygen target for the study of the $^{16}\text{O}(p,n)^{16}\text{F}$ reaction.¹⁵ Since it is not recommended to pump pure O_2 with the turbomolecular pumps of the jet target, we found that an H_2O vapor jet would be a feasible solution. Its development is described in section 3 below.

Finally, the previously reported¹⁶ method of measuring gas jet density profiles with ionizing electron beams has been employed for the study of predicted differences between jets mono- and diatomic gases. A report on these experiments follows in section 4.

2. The storage cell target setup in the Cooler A section

F. Sperisen, J. Doskow, H.O. Meyer, S.F. Pate, B. v. Przewoski, T. Rinckel, and A. Ross, IUCF, Bloomington, IN 47408

W. Haeberli and W.K. Pitts, Univ. of Wisconsin, Madison, WI 53706

Storage cells will be needed to provide useful thicknesses of *polarized* hydrogen and ^3He targets because of the relatively low flux available from sources of polarized atoms (up to about 10^{17} atoms/s, three orders of magnitude less than the flux in our gas jet). The storage cell is a tube aligned with the ion beam. Atoms are introduced into the cell at the midpoint along its length, and are constrained by the cell to a small volume around the beam until they escape and are pumped away. The achievable gas thickness decreases proportionally with the conductance, thus the cross-sectional area of the cell should be minimized. From that point of view, the Cooler A section, with no dispersion and relatively small beam aperture functions ($\beta_x=0.86$ m, $\beta_y=1.63$ m), turns out to be the best place for storage cell target experiments.

Figure 1 shows the setup installed in April 1991 in the A section. It consists of a two-stage differential pumping system, made up of three chambers from the Cooler Target Lab inventory. Integrated into the upstream stage are vertical and horizontal beam position monitors. The storage cell, located in the inner stage, is an aluminum tube of circular cross-section, 8 mm ID and 24 cm length. On either side there is a 1.5 μm thick mylar window, 5 mm high and 22.5 cm long; this makes it possible to detect low energy recoil protons from small angle pp elastic scattering. They are detected with three μ -strip detectors in coincidence with the forward going protons which exit the vacuum through a 0.13 mm thick stainless steel foil.

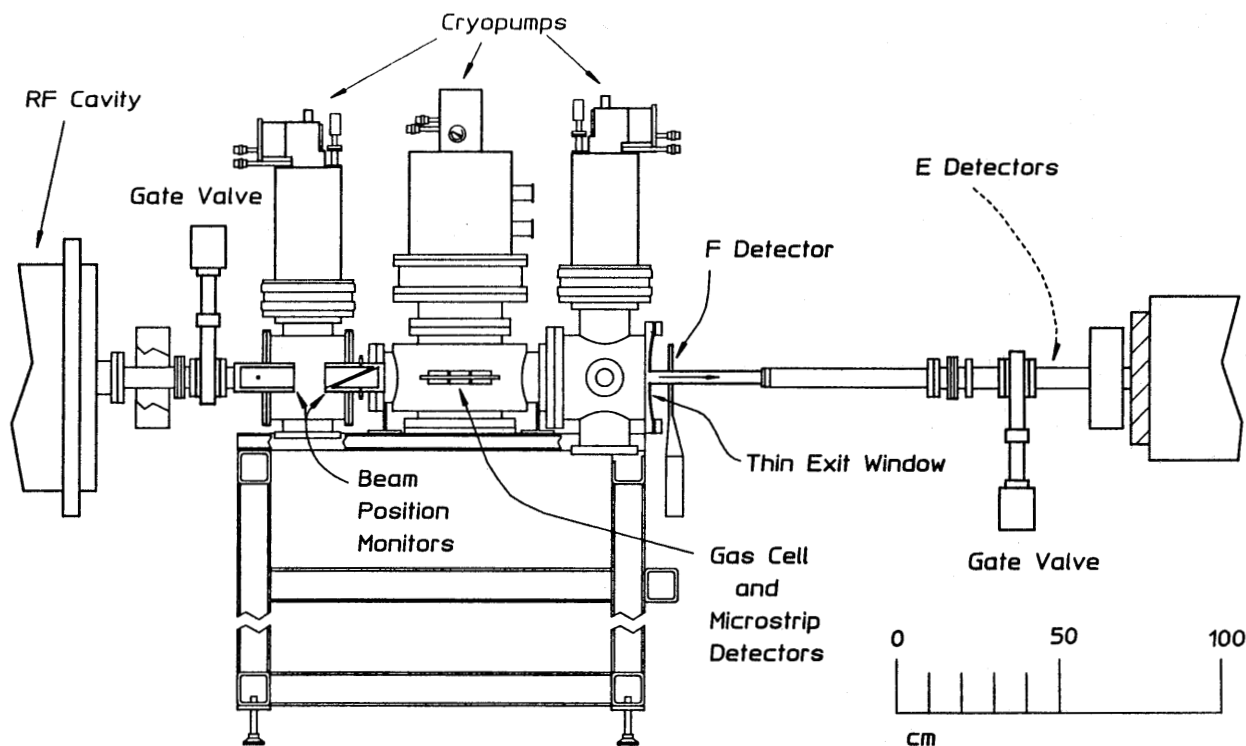


Figure 1. The storage target cell setup in the Cooler A section.

The gas is fed into the cell at its midpoint at flow rates comparable to those expected from polarized sources. A separate tube connects a capacitance pressure sensor (MKS 390 Baratron) to the midpoint of the cell, capable of measuring the pressure to within $4 \mu\text{Torr}$, corresponding to a target thickness of less than 2×10^{12} molecules/cm². The gas flow control system of the jet target⁵ was used with some minor modifications, allowing for fast turn-on/off, remote flow control, as well as flow rate measurement.

Each differential pumping stage is pumped by a cryo pump: The inner stage by a Leybold RPK 3000S12, the outer two stages each by a CTI Cryo-Torr 8, borrowed from our lab's HIPIOS project. The inner stage is separated from the outer stages by foil apertures, 12 mm wide by 16 mm high, corresponding to a machine acceptance of $35 \pi \mu\text{m}$. For a hydrogen flow rate of 1×10^{17} molecules/s into the cell, the target thickness, given by the measured pressure at the cell's midpoint, is 4.4×10^{14} molecules/cm². The pressures, measured by ion gauges, are 0.85 and $0.09 \mu\text{Torr}$ in the inner and outer stages, respectively. For a helium flow at the same rate the target thickness is 5.7×10^{14} atoms/cm², while the pressures in the pumping stages are 1.5 and $0.18 \mu\text{Torr}$.

An initial CE-26 run using this setup took place in May 1991. For a description of this run and its results see elsewhere in this report.¹³ We would like to thank J. Hudson, R. Palmer and R. Stillabower for their help with the installation, and M. Ball, T. Ellison, B. Hamilton and T. Sloan for their assistance with the beam position monitors.

3. Development of an H₂O jet target

T.W. Bowyer, F. Sperisen, J. Doskow, and J. Wellman

The $0^+ \rightarrow 0^-$ transition using the $^{16}\text{O}(p,n)^{16}\text{F}$ reaction is to be investigated in CE-19.¹⁵ Since thin internal targets must be used in the IUCF Cooler, a gaseous form of oxygen is desired for this experiment. Due to the corrosive and potentially damaging effects pure O₂ would apparently have on the turbomolecular pumps¹⁷ of the existing jet target, O₂ can not be used, so some alternate source of oxygen in gaseous form is needed. The only stable gas which contains oxygen without contaminants that might mock up the signature of the CE-19 experiment (coincident detection of low energy decay protons with fast neutrons), or create a background is H₂O vapor. The presence of hydrogen in the water molecule has the additional important advantage over the O₂ target that the luminosity can be monitored by *pp* elastic scattering as has been done successfully in Cooler experiments with H₂ targets.^{1,3,4}

We have been studying the feasibility of an H₂O jet target with a test setup as shown in Fig. 2. The method for jet formation and gas transport is essentially the same as used in the existing jet target.⁵ Water in a small copper reservoir is heated to a temperature corresponding to the desired vapor pressure, which in turn determines the flow rate through the nozzle and the jet thickness. A solenoid three-way valve allows for fast (40 ms) turn-on and turn-off of the jet; the line to the nozzle can be switched either to the H₂O reservoir (jet on) or to a pump (jet off). The path of the vapor from the reservoir to the nozzle has to be kept at or above the temperature of the reservoir in order to avoid condensation.

The H₂O jet expands through a Laval-type nozzle (throat diameter: 0.13 mm, exit diameter: 0.87 mm) into a vacuum chamber, pumped by a 1500 l/s turbo pump, and is caught by a cone-shaped catcher separated from the nozzle by an adjustable distance of

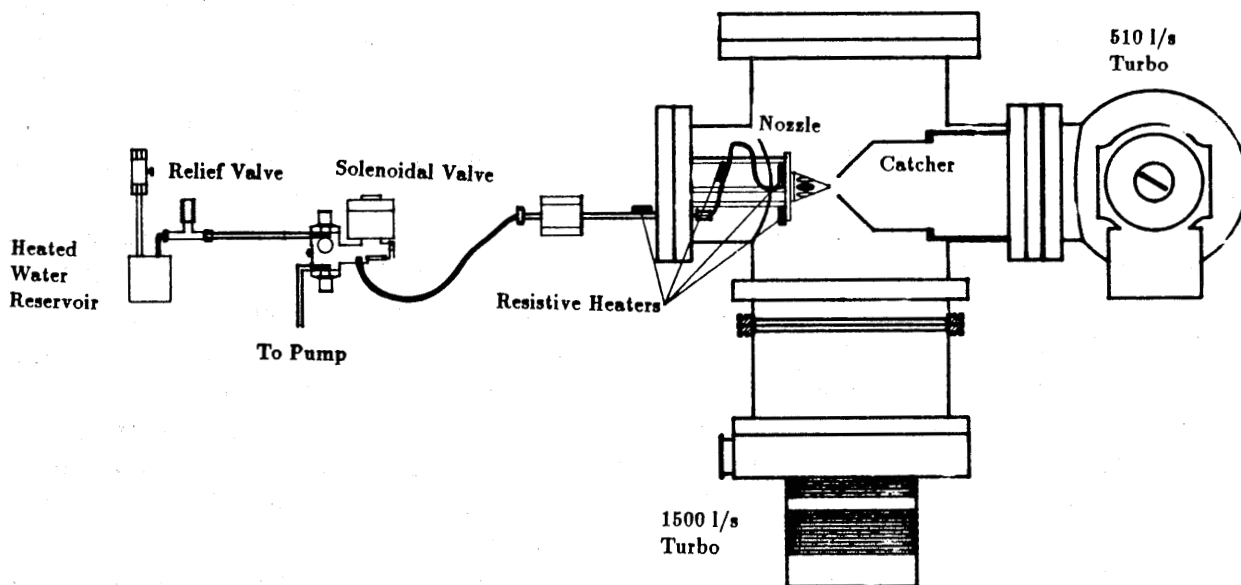


Figure 2. H₂O vapor jet test setup. Gaseous H₂O is transported through heated tubing, a solenoidal valve, and then through a heated nozzle.

5-20 mm, and pumped by a 500 l/s turbo pump. The fraction of the jet flow caught by this catcher can be determined by measuring the ratio of the chamber pressure with the catcher open and closed (assuming constant pumping speed of the 1500 l/s turbo pump). The flow rate is determined from the chamber pressure measured with an ion gauge (while the catcher is closed), and the known pumping speed. Furthermore, in our test apparatus we can measure the thickness profile of the jet, by scanning it with a 1 keV ionizing electron beam, while collecting and monitoring the ion current.¹⁶

The measured flow rates are in reasonable agreement with the values expected from the vapor pressure and calculated nozzle flow. Comparing catching fraction measurements between H₂O and N₂ jets, we found similar results (65% for H₂O as compared to 70% for N₂ with a nozzle-catcher separation of 10 mm and catcher opening diameter of 29 mm). Figure 3 shows a thickness profile of H₂O measured 2 mm from the nozzle, with a flow rate of 1.0×10^{19} molecules/s. The temperature of the water in the reservoir was 52 °C, corresponding to a vapor pressure of 93 Torr. The thickness given in Fig. 3 is based on the published¹⁸ H₂O ionization cross section of $7.7 \times 10^{-17} \text{ cm}^2$ for 1 keV electrons. Theoretical calculations based on one-dimensional compressible flow theory¹⁹ give a peak thickness of 1.3×10^{15} molecules/cm² which agrees well within uncertainties.

Water vapor can be pumped very efficiently by condensation on cold surfaces (cryo pumping). We have therefore carried out a test, replacing the 1500 l/s turbomolecular pump by two copper panels cooled by the two stages (80 °K and 20 °K) of a closed-cycle helium refrigerator. Measurements showed a pumping speed of ≥ 1500 l/s, approximately twice that of the turbomolecular pump. We plan to make a similar cryo pump for the first pumping stage of the actual H₂O jet target in the Cooler ring.

So far, a total amount of about 200 g of water has been pumped during our tests with no obvious effect on the pump performance. Our test results demonstrate the feasibility of an H₂O jet target for the Cooler. Optimum thicknesses (i.e., thicknesses of about 10^{14} molecules/cm², maximizing Cooler luminosity) should be easily achieved. Relatively minor modifications on the existing jet target setup will be needed to accommodate the H₂O jet.

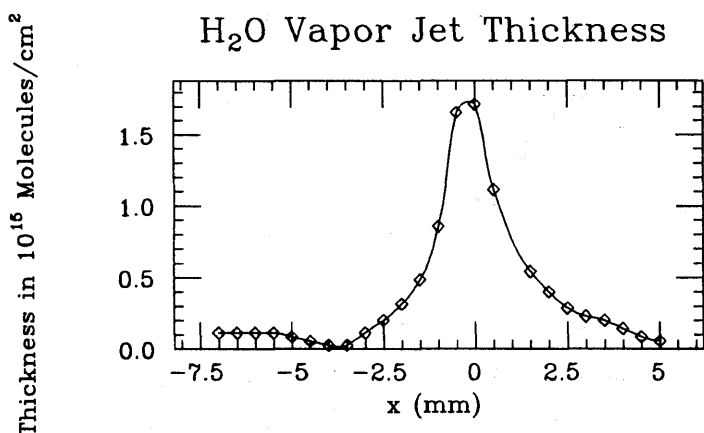


Figure 3. H₂O jet thickness profile obtained by ionization with a 1 keV electron beam at 2 mm from the nozzle. The gas flow rate was 1.0×10^{19} molecules/s.

4. Study of mono- and diatomic gas jets with electron beams*

J. Wellman, F. Sperisen, and J. Doskow

Further development of the existing IUCF gas jet target would benefit many experiments. To aid such development a good knowledge and understanding of the jet properties are needed. A method using ionizing electron beams to measure the density profile of gas jets has been developed recently at this lab.¹⁶ We have utilized this method to test calculations predicting that the jet opening angle of a diatomic gas is a factor of two larger than that of a monoatomic gas.

Jets emerging from a Laval-type nozzle (throat diameter: 0.23 mm; exit diam.: 1.92 mm) were scanned transversely with a 1 keV electron beam at various distances z from the nozzle. The nozzle was movable longitudinally from outside the vacuum chamber. The ions were collected with a ring-shaped copper electrode, 4 cm in diameter, surrounding the jet 1.5 cm downstream from the electron beam, biased at -60 V. The contribution from background gas ionization was measured by bleeding gas into the chamber through an inlet far from the nozzle, maintaining the same background pressure (typically 2×10^{-4} Torr). The electron beam current (typically $3 \mu\text{A}$) and its density profile was obtained by scanning the beam across a tantalum plate (biased at $+60$ V), and through a 0.3 mm hole in the middle onto a second collector behind it. The *total* ionization cross section σ is defined in terms of the ion current I_i , the electron current I_e , and the thickness t of the gas (density integrated along the e-beam) through $I_i/I_e = t\sigma$. Using published²⁰ values for σ , we were able to determine t . Argon was chosen as monoatomic and nitrogen as diatomic gas because they are easy to handle, have relatively large σ and are inexpensive.

Figure 4 shows N_2 jet profile scans (background subtracted) at three distances z from the nozzle tip. The overall systematic error for these results is estimated to be approximately 20%. The width (FWHM) of these peaks, as well as those obtained with

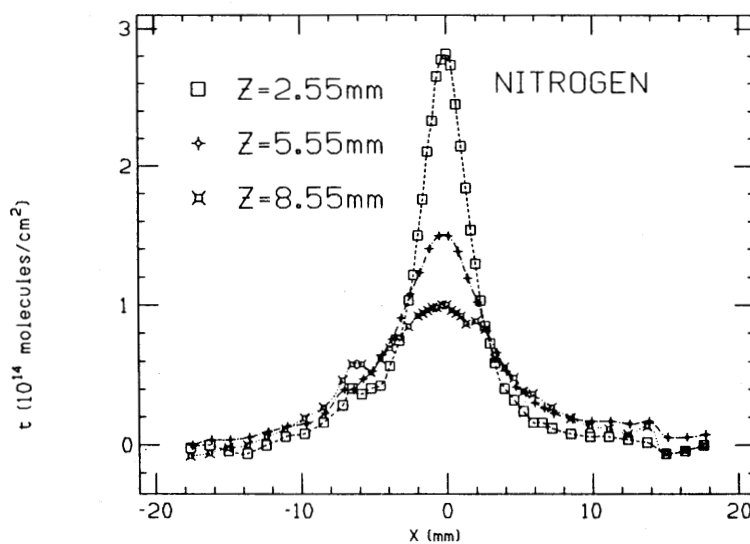


Figure 4. N_2 jet thickness profiles obtained by ionization with a 1 keV electron beam at three different distances z from the nozzle. The gas flow rate was 5.0×10^{18} atoms/s.

argon, are plotted vs. z in Fig. 5. The solid and dashed curves are linear fits, corresponding to full jet opening angles Φ of $47^\circ \pm 4^\circ$ and $54^\circ \pm 7^\circ$ for Ar and N_2 , respectively. These results are in clear disagreement with the predictions of a calculation based on one-dimensional compressible flow theory:¹⁹ $\Phi_{Ar} = 62^\circ$ and $\Phi_{N_2} = 120^\circ$. In Fig. 6 the measured N_2 peak jet thicknesses (at $x=0$) are plotted as function of the distance z from the nozzle. Error bars shown reflect the distribution of results of repeated measurements. Not shown is an estimated 20% systematic uncertainty. Calculations based on ref. 19 predict the thickness at the nozzle exit. We then assume that the jet expands at constant velocity and opening angle Φ to calculate the thickness outside the nozzle. Using the measured value for Φ_{N_2} (54°), we get the solid curve in Fig. 6, which agrees with the measured values within their systematic uncertainty, while the dotted curve, resulting from the theoretical opening angle, $\Phi_{N_2} = 120^\circ$, predicts too small thicknesses. A similar result has been obtained for argon, only there the difference between the two curves is smaller because of the smaller discrepancy between measured and calculated opening angle.

In conclusion, we have shown that the jet opening angle for argon and nitrogen jets are equal (within the experimental error) and smaller than predicted. The failure of the theory is particularly striking with respect to the predicted large (factor of 2) difference in the opening angle for mono- vs. diatomic gases. On the other hand, the theory does well in predicting the jet thickness at the nozzle exit. More detailed studies will be necessary in order to reduce the systematic uncertainties.

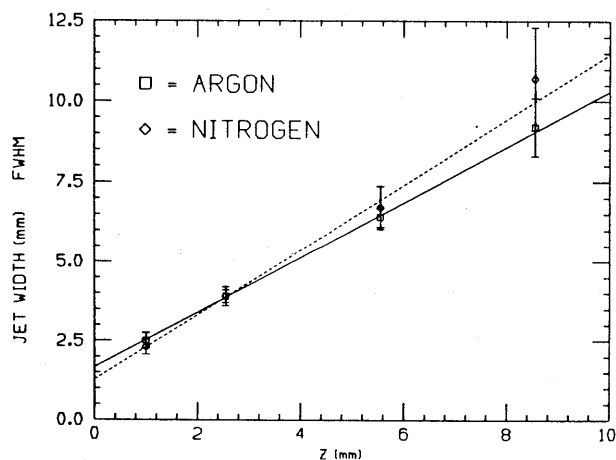


Figure 5. The width (FWHM) of Ar and N_2 jet profiles as a function of distance z from the nozzle. The solid and dashed curves are linear fits, determining the jet opening angle.

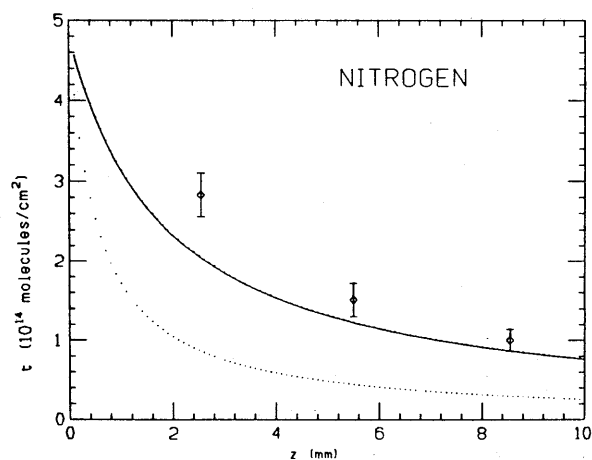


Figure 6. N_2 peak jet thicknesses (at $x=0$, Fig. 4) as a function of the distance z from the nozzle. The curves are predictions based on the measured (solid curve) and theoretical (dotted curve) jet opening angle.

* This work was part of the 1990 Research Experiences for Undergraduates Program.

1. H.O. Meyer, *et al.*, Phys. Rev. Lett. **65**, 2846 (1990).
2. W.K. Pitts, *et al.*, (CE-08), IUCF Scientific and Technical Report, May 1990–April 1991.
3. H.O. Meyer, *et al.*, (CE-23), IUCF Scientific and Technical Report, May 1990–April 1991.
4. W. Daehnick, *et al.*, (CE-03), IUCF Scientific and Technical Report, May 1990–April 1991.
5. F. Sperisen, *et al.*, IUCF Scientific and Technical Report, January 1987 - April 1988, p. 194.
6. F. Sperisen, *et al.*, IUCF Scientific and Technical Report, May 1989 - April 1990, p. 117.
7. R.E. Pollock, *et al.*, (CE-17), IUCF Scientific and Technical Report, May 1990–April 1991.
8. B. von Przewoski, *et al.*, (CE-18), IUCF Scientific and Technical Report, May 1990–April 1991.
9. M.G. Minty, *et al.*, IUCF Scientific and Technical Report, May 1989 - April 1990, p. 121.
10. P.V. Pancella, *et al.*, IUCF Scientific and Technical Report, May 1989 - April 1990, p. 123.
11. P.V. Pancella, *et al.*, IUCF Scientific and Technical Report, May 1989 - April 1990, p. 125.
12. F. Sperisen, *et al.*, IUCF Scientific and Technical Report, May 1989 - April 1990, p. 127.
13. W. Haeberli, *et al.*, (CE-26), IUCF Scientific and Technical Report, May 1990–April 1991.
14. J. Sowinski and J. van den Brand, spokespersons, "Investigation of the ^3He wave function by quasi-free scattering," IUCF Proposal No. 90-111, October 1990.
15. T.W. Bowyer and S.E. Vigdor, spokespersons, "Study of the $^{16}\text{O}(p,n)^{16}\text{F}(0^-)$ Reaction at $T_p = 300$ MeV in the IUCF Cooler", IUCF Proposal No. 90-07, June 1990.
16. H. Hardner and F. Sperisen, IUCF Newsletter **45**, 26 (1989).
17. R. Hellmer, Balzers High Vacuum Prod., private communication.
18. A. Zecca, *et al.*, J. Phys. B: At. Mol. Phys. **20**, L133 (1987).
19. J.A.D. Ackroyd, SRC Daresbury Rep. DL/NSF/R12 (1975).
20. L.J. Kiefer and G.H. Dunn, Rev. Mod. Phys. **38**, 1 (1966).